Theoretical Design of High-Dual-Sensing-Performance Sensors Based on a Magnetoplasmonic Nanostructure

Xiaofeng Bai[a, b*], Jingjing Sun[a], Yupan Yun[c*]

[a] Library, Hebei GEO University, Hebei GEO University, No. 601, Hebei Avenue, Shijiazhuang 052161, People's Republic of China.

[b] Hebei Key Laboratory of Optoelectronic Information and Geo-detection Technology, Hebei GEO University, No. 601, Hebei Avenue, Shijiazhuang 052161, People's Republic of China.

[c] School of Water Resources and Environment, Hebei Centre for Ecological and Environmental Geology Research, Hebei GEO University, No. 601, Hebei Avenue, Shijiazhuang 052161, People's Republic of China.

Traditionally, the Fano-like spectrum can be fitted using the following equation:

$$I_{T-MOKE} = A + B * \frac{\left(\frac{\gamma\Gamma}{2} + P - P_r\right)^2}{\left(\frac{\Gamma}{2}\right)^2 + \left(P - P_r\right)^2}, \quad (1)$$

where I_{T-MOKE} represents the amplitude of the T-MOKE spectrum. The fitting parameters A and B correspond to the background and the overall peak height, respectively. P_r denotes the wavelength or angle of incidence at the resonant position, while γ is the Breit–Wigner Fano parameter that determines the asymmetry of the spectrum near this resonant position. Γ is the linewidth of the T-MOKE curve. Figs. S1, S2, and S3 illustrate the fitting of the spectra shown in Figs. 3b, 4a, and 4b of the manuscript, respectively. The corresponding parameters are detailed in Tables S1, S2, and S3. Evidently, all the T-MOKE results exhibit an excellent fit, which validates the analysis of the T-MOKE with respect to the Fano-like shape. Specifically, for the reflectance spectra presented in Fig. 4a of the manuscript, we focused on the second dip (i.e., the value of P_r) in eq (1)) in the reflectance curve, which is attributed to surface plasmon

resonance (SPR) excitation, to evaluate the sensor's performance. Additionally, this fitting approach provides a comprehensive understanding of the interaction mechanisms at play, enabling more accurate predictions of sensor behavior under various conditions. The precision of this model underscores its importance in the design and optimization of advanced sensor systems.

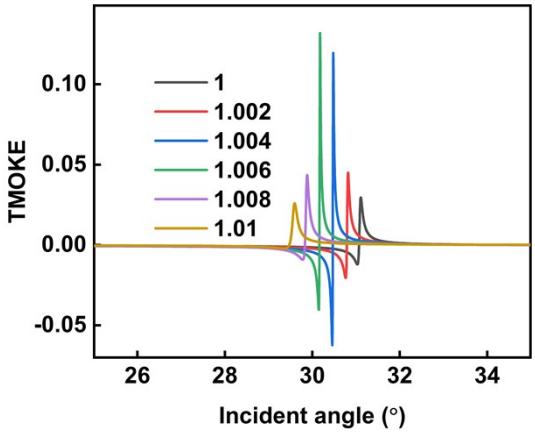

Fig. S1 Fits of the Fano line shapes presented in Fig. 3b, with the fitting linewidth values for the different curves provided in Table S1.

Table S1 Fitting parameter values for the T-MOKE curves shown in Fig. S1

Refractive index	Linewidth (°)	A	B	γ
1	0.072	-0.01199	0.01172	1.595
1.002	0.051	-0.02042	0.02009	1.502
1.004	0.022	-0.06229	0.06187	1.392
1.006	0.024	-0.04028	0.03986	1.821
1.008	0.119	-0.009156	0.008821	2.23
1.01	0.132	-0.01199	0.01172	1.595

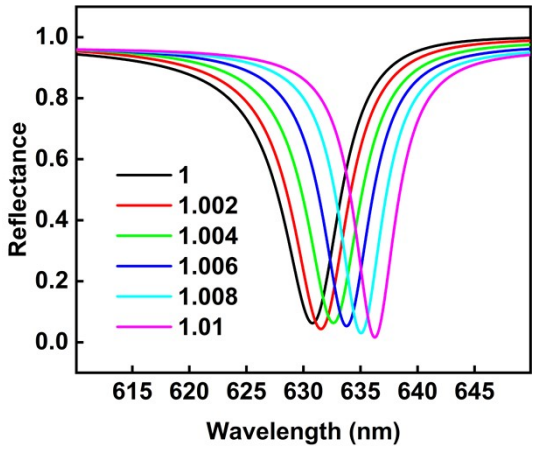

Fig. S2 Fits of the Fano line shapes shown in Fig. 4a, with the fitting linewidth values for the different curves detailed in Table S2.

Table S2 Fitting parameter values for the reflectance curves displayed in Fig. S2.

Refractive index	Linewidth (nm)	A	B	γ
1	6.058	0.06232	0.9276	0.1053
1.002	5.869	0.04322	0.9496	0.07551
1.004	5.677	0.06309	0.9214	0.05224
1.006	5.098	0.05271	0.9226	0.0301
1.008	4.621	0.02981	0.9389	0.0111
1.01	4.38	0.01598	0.9499	0.0003246

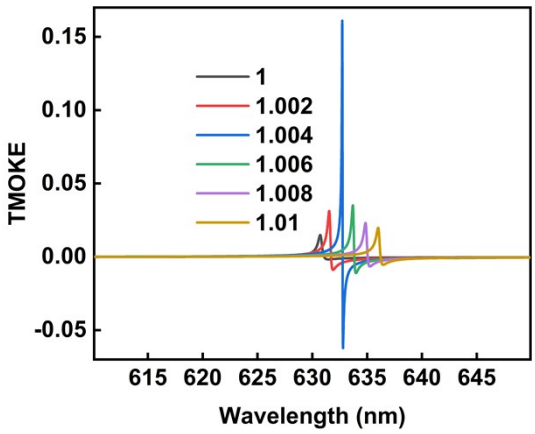

Fig. S3 Fits of the Fano line shapes in Fig. 4b, with the fitting linewidth values for the different curves detailed in Table S3.

Table S3 Fitting parameter values for the T-MOKE curves shown in Fig. S3.

Refractive index	Linewidth (nm)	A	B	γ
1	0.4358	0.001487	-0.01506	0.3194
1.002	0.2849	0.03129	-0.0315	0.5228
1.004	0.06113	0.1611	-0.1613	0.6199
1.006	0.2364	0.03505	-0.03521	0.5553
1.008	0.3285	0.02307	-0.02322	0.5229
1.01	0.3671	0.01975	-0.01989	0.5138